Nucleic Acids Research, 1998, Vol. 26, No. 18 **4173–4177**

Thermodynamic and kinetic studies of the formation of triple helices between purine-rich deoxyribo-oligonucleotides and the promoter region of the human c-*src* proto-oncogene

Palok Aich, Shawn Ritchie[1], Keith Bonham[1] and Jeremy S. Lee*

Department of Biochemistry, University of Saskatchewan, 107 Wiggins Road, Saskatoon, SK S7N 5E5, Canada and [1]Saskatoon Cancer Research Unit, 20 Campus Drive, Saskatoon, SK S7N 5E5, Canada

Received May 27, 1998; Accepted July 23, 1998

ABSTRACT

The thermodynamic and kinetic parameters of triplex formation between four purine-rich oligonucleotides and a 22 bp pyrimidine·purine tract in the promoter region of the c-*src* gene were determined by fluorescence polarization studies. Three of these four oligonucleotides were 11 nt in length, corresponding to the left, central or right portion of the tract, while the fourth was a 22mer covering the whole tract. Binding constants (K_a) were measured as a function of Mg^{2+} concentration (0–10 mM) and temperature (0–41°C). In 10 mM Mg^{2+}, K_a for the left, central and right 11mers were 0.26, 0.75 and 1.4 × 10^8/M, respectively, while for the 22mer the value was 1.8 × 10^8/M at 22°C. Under the same conditions, K_a was estimated by an electrophoretic band shift technique. The agreement between the two methods was acceptable for the 22mer but not for the 11mers. Kinetic measurements demonstrated that the rate of dissociation of the 22mer from the triplex was significantly slower than that of the 11mers, providing an explanation for the observed discrepancy. The entropy and enthalpy of triplex formation were calculated from van't Hoff plots. In all cases the entropy was favourable, especially for the 22mer and for the 11mer with the lowest guanine content. The enthalpy was unfavourable for the 22mer and most favourable for the 11mer with the highest guanine content. These results provide a thermodynamic explanation for length and sequence effects on the formation of purine·pyrimidine·purine triplexes.

INTRODUCTION

The thermodynamics of duplex formation have been well-documented (1–6). On the other hand, triplexes have received much less attention and inconsistencies are apparent in the reported values of some thermodynamic parameters (7–18). Nor can the underlying principles of triplex formation be deduced from the behaviour of duplexes, because in many cases their properties are very different. For example, duplexes are stabilized by monovalent cations, whereas pyr·pur·pyr triplexes containing a large proportion of C·G·C^+ base triads are destabilized by increasing the ionic strength (19–26). Similarly, the formation of pur·pyr·pur triplexes is inhibited by K^+ and depends on the presence of a divalent cation; requirements which do not apply to duplexes (27–30). Yet understanding the thermodynamics of triplex formation is important for the rational design of oligonucleotides for use in antigene therapeutic applications (31 and references therein). For this reason, we have studied the interaction between oligonucleotides and a 22 bp pyr·pur tract (named TC1) which occurs in the promoter region of the c-*src* human proto-oncogene (32).

The human c-*src* gene is the normal homologue of the transforming gene of Rous sarcoma virus (32). The c-*src* gene encodes a non-receptor tyrosine kinase, $pp60^{c\text{-}src}$, a member of a group of several closely related enzymes that are activated in a number of human cancers (33,34). Analysis of the promoter region of the c-*src* gene has shown that it contains four pyr·pur tracts within ~120 bp and this region is critical for promoter activity (32). Mutation or disruption of these tracts, including TC1, leads to significant reductions in the level of transcription (K.Bonham, unpublished). Therefore, TC1 is a potential target for the binding of oligonucleotides to modulate the activity of this gene. In this report, the binding of eight oligonucleotides to a TC1 duplex was assessed by fluorescence polarization. The relevant sequences are shown in Figure 1. The modelled pyr·pur duplex was flanked by four GC-rich base pairs at each end to minimize the likelihood of forming alternative structures. All of the oligonucleotides were labelled with fluorescein at the 5′-end. We used an antiparallel 22mer purine (Aap) that spans the whole of TC1, three antiparallel 11mer purines that correspond to the sequence of the left (AapL), center (AapCen) and right (AapR) portions of TC1 and another 11mer of the same sequence as AapR except that all adenosines were substituted by thymines (TapR). The above sequences are all in antiparallel orientation with respect to the purine strand of the duplex. Three other 11mers with a parallel orientation corresponding to the right end of the duplex were studied; the purine 11mer ApRR and two pyrimidine 11mers TCR and TmCR, the latter containing 5-methylcytosine.

In general, the binding of oligonucleotides to duplex DNA has been studied by band shift techniques or by chemical modification (35,36). Unfortunately, in these methods the amount of triplex formation cannot be measured under equilibrium conditions, so that binding or kinetic parameters can only be estimated and

*To whom correspondence should be addressed. Tel: +1 306 966 4371; Fax: +1 306 966 4390; Email: leejs@sask.usask.ca

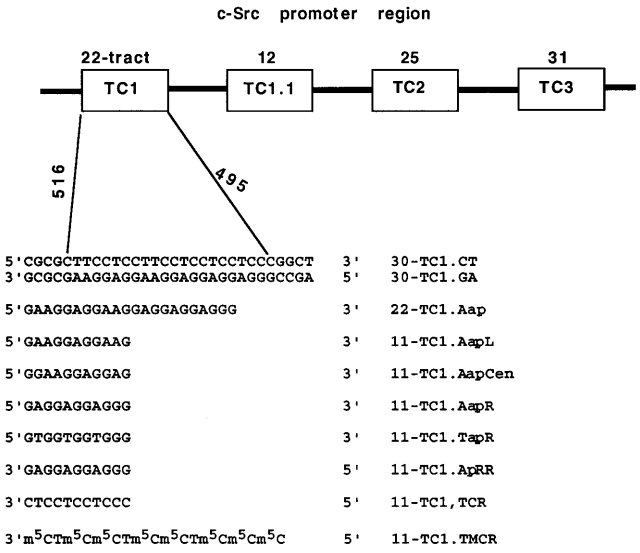

Figure 1. Schematic diagram of the relative positions of the c-*src* promoter regions and the sequences of the oligonucleotides.

comparisons between different sequences or counterions become difficult. On the other hand, fluorescence polarization measurements can be performed under equilibrium conditions. The polarization of the fluorescein-labelled oligonucleotides is determined by the size of the molecule to which the fluorescein is attached (37). Therefore, upon triplex formation with the larger duplex the polarization increases. By titrating the oligonucleotide with increasing concentrations of duplex, isotherms can be constructed from which binding parameters can be extracted (38–41). The technique is rapid, versatile and can be performed at various temperatures so that thermodynamic and kinetic information is also available.

MATERIALS AND METHODS

Oligonucleotides

All oligonucleotides were purchased from the Regional DNA Synthesis facility of the University of Calgary. They were gel purified before use. Where applicable the fluorescein label was introduced at the 5′ position with Pharmacia Fluoroprime™. The TC1 duplex was annealed in 20 mM HEPES, pH 7.0, 10 mM NaCl. The ethidium fluorescence assay was used to ensure complete duplex formation as described previously (42).

Triplex formation

Fluorescence polarization studies were performed with a bioluminescent polarimeter (PanVera Corporation). A fixed concentration of fluorescein-labelled oligonucleotide (2 nM) in 1 ml standard buffer (20 mM HEPES, pH 7.0, 10 mM NaCl with 0–10 mM Mg^{2+}) was titrated against increasing concentrations of TC1 duplex. The millipolarization value (*mP*) was measured at equilibrium (usually within 30 min). The association constant (K_a) was determined by fitting the data to the single site binding isotherm

$$mP = (mP_{max}\cdot K_a\cdot[\text{duplex}]_f - mP_{min})/(1 + K_a\cdot[\text{duplex}]_f) \quad \mathbf{1}$$

with Deltaplot™. The correlation coefficient (r^2) was >0.9 in all cases.

Band shift assay

The duplex target TC1 was annealed from single-stranded oligonucleotides in 10 mM Tris–HCl, pH 8.0, 1 mM EDTA and 100 mM NaCl at 100°C followed by slow cooling to room temperature. Duplexes were labelled with [α-^{32}P]dCTP using Klenow fragment followed by purification on Stratagene push columns.

Binding reactions containing oligonucleotides in the standard buffer with 10 mM Mg^{2+} were heated to 65°C for 10 min and quickly cooled before being annealed to the labelled duplex target. Typical reactions consisted of oligonucleotides (0.135–13.5 pmol) in 0 and 100 times molar excess over the duplex (0.135 pmol, 50 000 c.p.m.). Following incubation at room temperature for 2 h, the products were resolved on a 12% polyacrylamide gel for 1450 V h (100 V for 14.5 h) in standard buffer with 10 mM Mg^{2+}. The gel was visualized by autoradiography. The percent of total duplex target bound by the oligonucleotide in each lane of the band shift assay was quantified by densitometry analysis and calculated as follows:

% triplex DNA = triplex band density/(triplex band density + duplex band density).

The data were curve fitted to evaluate the equilibrium K_a as follows:

$$\%\ \text{triplex} = ([\text{TFO}]\cdot K_a)/(1 + [\text{TFO}]\cdot K_a) \quad \mathbf{2}$$

Thermodynamic parameters

The value of the free energy at 25°C was evaluated from $\Delta G^\circ_{25} = -298\cdot R\ln K_a$, where R is the universal gas constant. K_a was measured at six different temperatures between 0 and 41°C.

$$\ln K_a = -(\Delta H^\circ/RT) + (\Delta S^\circ/R) \quad \mathbf{3}$$

Therefore, the slope of a plot of $\ln K_a$ versus $1/T$ (van't Hoff plot) yields ΔH° (the standard enthalpy change).

Kinetic parameters

The kinetics of triplex formation at 20°C was monitored by adding a 5-fold excess of duplex to a fluorescein-labelled oligonucleotide at three different concentrations of Mg^{2+}, 2, 5 and 10 mM. The first *mP* value was measured within 20 s and then every 15 s thereafter. In every case, the rate of formation could be fitted with a single exponential expression of the following type (11):

$$y = a \times [1 - \exp(-x/t_{1/2})] \quad \mathbf{4}$$

where *y* is the fraction of triplex formed, *x* is the time in seconds, *a* is the amplitude of the interaction and $t_{1/2}$ denotes the time required to form 50% of the triplex.

RESULTS

Triplex formation was assessed by steady-state fluorescence polarization studies as shown in Figure 2 for four of the oligonucleotides. For each Mg^{2+} concentration, the concentration of duplex required to reach the mid-point of the change in *mP* value is ~$1/K_a$. Therefore, some differences in the binding of the oligonucleotides are apparent from visual inspection and the values of K_a determined from **1** are given in Table 1. For example, since the curves for Aap are displaced to the left compared with AapL, the former has the higher binding constant. Similarly, within the 11mers the order is AapR > AapCen > AapL at every Mg^{2+} concentration and this order follows the guanine content of the oligonucleotides; 8, 7 and 6, respectively. As well, the 22mer

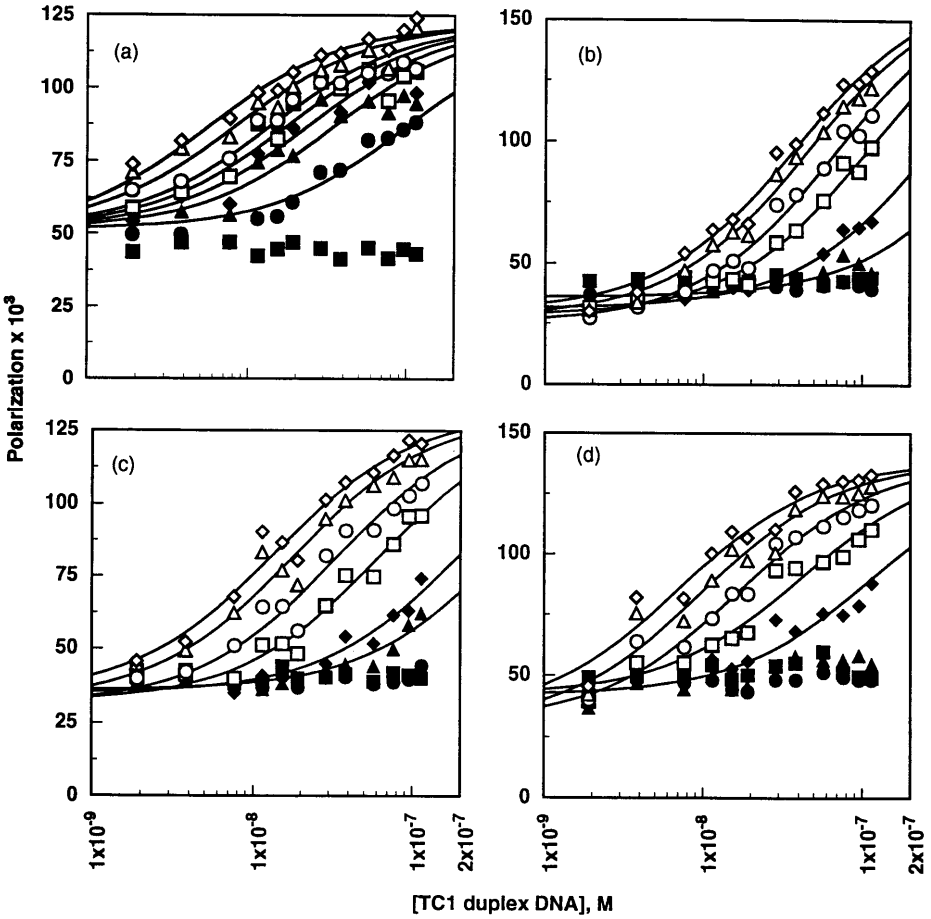

Figure 2. Triplex formation measured by fluorescence polarization. The *mP* value of the four fluorescein-labelled oligonucleotides increases upon addition of the TC1 duplex. (**a**) Aap; (**b**) AapL; (**c**) AapCen; (**d**) AapR. The Mg^{2+} concentrations were 0 (■), 0.1 (●), 0.3 (▲), 0.5 (◆), 1 (□), 2 (○), 5 (△) and 10 (◇) mM. Solid lines indicate the best fit curves based on the equation described in Materials and Methods.

Aap shows significant binding even at 0.1 mM Mg^{2+}, whereas the other three 11mers require higher concentrations. Two important controls were performed. First, there was no significant increase in *mP* value for any of the antiparallel oligonucleotides in the presence of calf thymus DNA. Second, the parallel 11mer homologous to the right end of the TC1 tract (ApRR) also showed no binding to the TC1 duplex under these conditions. Therefore, binding requires the correct orientation and sequence homology between the purine oligonucleotide and the pyr·pur tract.

Table 1. Association constants (K_a) at 22°C

[Mg^{2+}] (mM)	K_a (per M, ×10^8) AapL	AapCen	AapR	Aap
0.1	n.b.[a]	n.b.	n.b.	0.099 ± 0.02
0.3	0.014 ± 0.001	0.03 ± 0.0008	n.b.	0.28 ± 0.06
0.5	0.036 ± 0.004	0.05 ± 0.001	0.085 ± 0.02	0.42 ± 0.097
1.0	0.093 ± 0.009	0.16 ± 0.004	0.24 ± 0.065	0.57 ± 0.13
2.0	0.15 ± 0.015	0.3 ± 0.008	0.6 ± 0.16	0.72 ± 0.16
5.0	0.22 ± 0.02	0.6 ± 0.016	1.0 ± 0.27	1.2 ± 0.28
10.0	0.26 ± 0.03	0.75 ± 0.02	1.4 ± 0.378	1.8 ± 0.41

[a] n.b., no binding.

Three pyrimidine-containing oligonucleotides were also investigated, namely TapR (TG-containing), TCR (TC-containing) and TMCR (Tm^5C-containing), which were designed to bind to the right side of the TC1 tract (Fig. 1). None of these gave rise to a significant increase in *mP* value at the highest concentration of duplex which could be tested. Therefore, K_a is $<10^6$/M under the standard conditions. However, it should be noted that the fluorescence of fluorescein is quenched below pH 7, so that TCR and TMCR cannot be tested at low pH, conditions under which they would be expected to bind (30).

Binding of the four antiparallel purine oligonucleotides to TC1 was also assessed by a band shift assay in the standard buffer with 10 mM Mg^{2+} (14). As shown in Figure 3a, the presence of the 22mer Aap causes a reduction in the mobility of the TC1 duplex and triplex formation is essentially complete when the 22mer is in 20-fold excess. As described previously (14), K_a can be estimated from this data and was found to be 4×10^7/M. This value is ~5-fold lower than was obtained by fluorescence polarization (Table 1). Band shifts for the 11mers AapR and AapL are shown in Figure 3b. In both cases the change in mobility on triplex formation is much less than with the 22mer and is only observed at the highest concentration of oligonucleotide. The 11mer AapCen gave similar results (data not shown). The K_a values were estimated to be of the order of 10^5/M, or about two

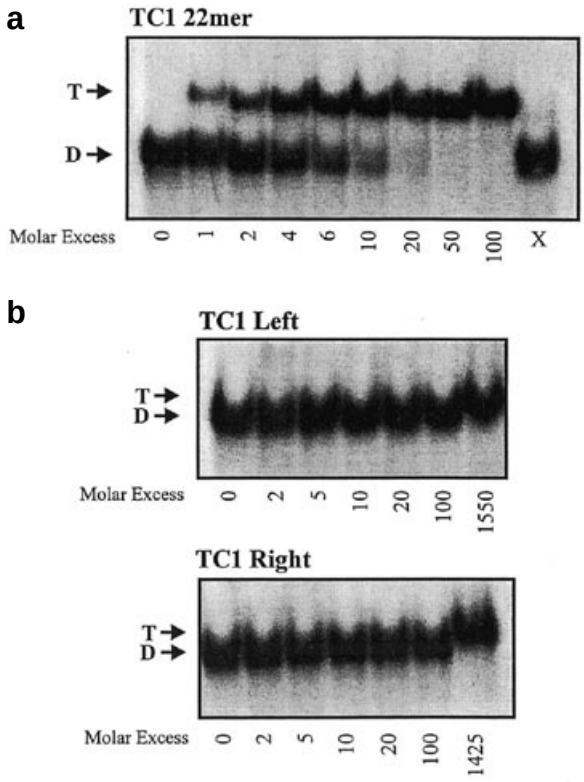

Figure 3. Band shift analysis of triplex formation within the TC1 duplex. (**a**) Aap; (**b**) (top) AapR and (bottom) AapL. The concentrations (in molar excess above target concentration) are shown below each lane. Arrows mark the positions of duplex (D) and triplex (T) bands. X indicates a control of the parallel purine oligonucleotide 22mer at a 400 molar excess.

orders of magnitude lower than derived by fluorescence polarization (Table 1).

The thermodynamics of triplex formation in 10 mM Mg^{2+} were investigated by measuring K_a as a function of temperature. The resulting van't Hoff plots are shown in Figure 4. For the 22mer the slope is negative, whereas the 11mers all have positive slopes. The calculated thermodynamic parameters are listed in Table 2. It is clear that in all cases, a favourable entropy term is important for driving triplex formation, especially for the 22mer, for which the enthalpy is actually unfavourable. AapR, which contains eight guanine residues, has the most favourable enthalpy compared with AapCen (seven guanines) and AapL (six guanines).

Table 2. Thermodynamic parameters

	ΔG°_{25} (kcal/mol)	ΔH° (kcal/mol)	ΔS° (e.u.)
Aap	–11.8	2.3	47.3
AapL	–10.5	–4.8	19.3
AapCen	–10.8	–5.2	18.7
AapR	–10.7	–7.65	10.3

The rate of triplex formation at three different Mg^{2+} concentrations was also measured by fluorescence polarization. As shown in Figure 5, at 2 mM Mg^{2+} formation of the triplex by the 22mer is much slower than for the 11mers. In all cases the $t_{½}$ decreases with increasing Mg^{2+} (Table 3). Amongst the 11mers, AapR, which has the highest guanine content, has the fastest on rate.

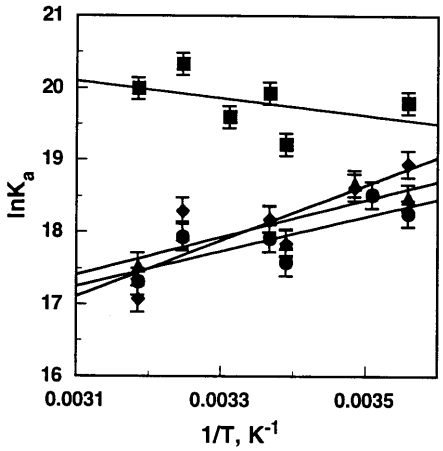

Figure 4. van't Hoff plots of lnK_a versus 1/T for the interactions between Aap (■), AapL (●), AapCen (▲), AapR (◆) and the TC1 c-*src* duplex. Solid lines denote the best linear fit.

Table 3. Kinetic constants for triplex formation

	$[Mg^{2+}]$ (mM)	a	$t_{½}$ (s)
Aap	2	0.73	463
	5	0.91	174
	10	0.93	19.8
AapL	2	0.95	78
	5	0.98	37.6
	10	0.98	19.3
AapCen	2	0.92	32
	5	0.93	16.5
	10	0.97	15.7
AapR	2	0.91	25.3
	5	0.96	8.5
	10	0.95	0.7

$t_{½}$ is the time required for 50% formation of triplex and a is the amplitude as defined in equation **4**.

DISCUSSION

In 10 mM Mg^{2+}, binding constants were measured by both fluorescence polarization and by band shift techniques. For the 22mer the agreement between the methods was acceptable, although the K_a from the band shift assay gave the lower value; for the 11mers, on the other hand, the band shift technique underestimated the K_a by ~2 orders of magnitude. The simplest explanation for this discrepancy is that the complex dissociates during the gel run, which takes many hours. The measured rate constants would also support this view. Since K_a is the ratio K_{on}/K_{off}, it can be calculated that the off rate for the 22mer is much slower than for the 11mers, so that dissociation during the gel run is more evident for the shorter oligonucleotides. Fluorescence polarization does not suffer from this problem because binding parameters are measured under equilibrium conditions.

The rate of complex formation is not only determined by length but also by the sequence of the 11mers. The fastest on rate is for Aapr, which has the highest guanine content. In general, G-rich oligonucleotides have strong stacking interactions which may lead to an ordered structure (35). The purine residues of the third strand are also stacked and ordered in the triplex. Therefore,

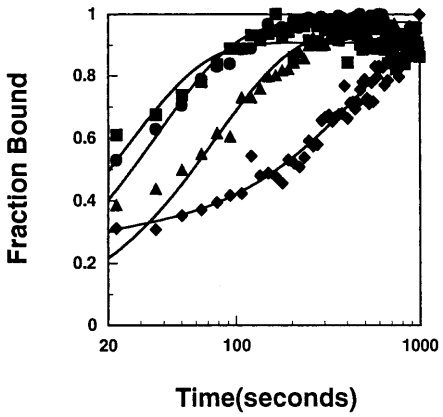

Figure 5. Fraction of triplex formed with time between Aap (◆), AapL (▲), AapCen (●), AapR (■) and the TC1 c-*src* duplex in 2 mM Mg^{2+}. Solid lines are the best fit curves using the equation described in Materials and Methods.

complex formation may require less rearrangement of the purine strand if it is G-rich, leading to a faster on rate.

The binding constant can also be considered in terms of enthalpy and entropy. For the 11mers, the enthalpy is again correlated with guanine content. As discussed above, this is most likely due to stronger stacking interactions in the triplex for G-rich oligonucleotides. On the other hand, the entropy term becomes less favourable with higher guanine content. Stacking interactions may also provide the explanation, since a G-rich oligonucleotide will already be well ordered in the unbound state. The net result of this enthalpy/entropy compensation is that the binding constant as a function of guanine content varies by less than an order of magnitude.

For the longer oligonucleotide, the enthalpy is unfavourable and the reaction becomes entropy driven. This may be due to considerable self-structure within the 22mer which must be disrupted before complex formation can occur. The slow on rate is consistent with this idea, as is the high entropy of complex formation. The net result is that a longer polymer does not show a considerable increase in binding constant, as would be expected in the case of duplex formation. Indeed, longer polymers may show a decrease in binding constant. For example, for oligopurines targeted to the c-K-*ras* promoter, binding constants for a 20mer and 30mer were 2.5×10^7 and 4×10^6/M, respectively (43). Therefore, a polymer of ~20 nt may be optimal in terms of binding affinity.

In conclusion, we have demonstrated that fluorescence polarization is an excellent technique for measuring thermodynamic and kinetic parameters. In comparison, band shift techniques tend to underestimate binding constants, especially for shorter oligonucleotides. It was found that there is enthalpy/entropy compensation as a function of both length and guanine content of the oligonucleotide. Therefore, there is an apparent upper limit for the binding constant to this tract in the c-*src* promoter of ~10^8/M, which may limit the usefulness of oligonucleotide-directed gene therapy.

ACKNOWLEDGEMENTS

This work was supported by the Medical Research Council of Canada and by HSURC with a fellowship to P.A.

REFERENCES

1 Bloomfield,V.A., Crothers,D.M. and Tinoco,I.,Jr (1974) In *Physical Chemistry of Nucleic Acids*. Harper and Row, New York, NY, p. 517.
2 Breslauer,K.J., Frank,R., Blöcker,H. and Marky,L.A. (1986) *Proc. Natl Acad. Sci. USA*, **83**, 3746–3750.
3 Felsenfeld,G. and Miles,H.T. (1967) *Annu. Rev. Biochem.*, **36**, 407–448.
4 Freir,S.M., Kierzek,R., Jaeger,J.A., Sugimoto,N., Caruthers,M.H., Neilson,T. and Turner,D.H. (1986) *Proc. Natl Acad. Sci. USA*, **83**, 9373–9377.
5 Klump,H.H. (1988) In Jones,M.N. (ed.), *Biochemical Thermodynamics*, 2nd Edn. Elsevier, Amsterdam, The Netherlands, pp. 100–144.
6 Saenger,W. (1984) In Cantor,C.R. (ed), *Principles of Nucleic Acid Structure*. Springer Verlag, New York, NY, p. 556.
7 Hopkins,H.P., Hamilton,D.D., Wilson,W.D., Campbell,J. and Fumero,J. (1993) *J. Chem. Thermodynam.*, **25**, 111–126.
8 Park,Y.-W. and Breslauer,K.J. (1992) *Proc. Natl Acad. Sci. USA*, **89**, 6653–6657.
9 Krakauer,H. and Sturtevant,J.M. (1968) *Biopolymers*, **6**, 491–512.
10 Neumann,E. and Ackerman,J. (1969) *J. Phys. Chem.*, **73**, 2170–2178.
11 Ross,P.D. and Scruggs,R. (1965) *Biopolymers*, **3**, 491–496.
12 Xodo,L.E., Manzini,G. and Quadrifoglio,F. (1990) *Nucleic Acids Res.*, **18**, 3557–3564.
13 Plum,E.G., Park,Y.-W., Singleton,S.F., Dervan,P.B. and Breslauer,K.J. (1990) *Proc. Natl Acad. Sci. USA*, **87**, 9436–9440.
14 Roberts,R.W. and Crothers,D.M. (1991) *Proc. Natl Acad. Sci. USA*, **88**, 9397–9401.
15 Ito,T., Smith,C.L. and Cantor,C.R. (1992) *Proc. Natl Acad. Sci. USA*, **89**, 495–498.
16 Brenowitz,M., Senear,D.F., Shea,M.A. and Ackers,G.K. (1986) *Methods Enzymol.*, **130**, 132–181.
17 Singleton,S.F. and Dervan,P.B. (1992) *J. Am. Chem. Soc.*, **114**, 6957–6965.
18 Shindo,H., Torigoe,H. and Akinori,S. (1993) *Biochemistry*, **32**, 8963–8969.
19 Yang,M., Ghosh,S.S. and Millar,D.P. (1994) *Biochemistry*, **33**, 15329–15337.
20 Durand,M., Peloille,S., Thuong,N.T. and Maurizof,J.-C. (1992) *Biochemistry*, **31**, 9197–9204.
21 Hopkins,H.P., Hamilton,D.D., Wilson,W.D. and Zon,G. (1993) *J. Phys. Chem.*, **97**, 6555–6563.
22 Kibler-Herzoz,L., Kell,B., Zon,G., Shinozuka,K., Mizan,S. and Wilson,W.D. (1990) *Nucleic Acids Res.*, **18**, 3545–3555.
23 Pilch,D.S., Brousseau,R. and Shafer,R.H. (1990) *Nucleic Acids Res.*, **18**, 5743–5750.
24 Rougee,M., Faucon,B., Mergny,J.L., Bercelo,F., Giovannangeli,C., Garestier,T. and Hélène,C. (1992) *Biochemistry*, **31**, 9269–9278.
25 Shea,R.G., Ng,P. and Bischofberger,N. (1990) *Nucleic Acids Res.*, **18**, 4859–4866.
26 Singleton,S.F. and Dervan,P.B. (1993) *Biochemistry*, **32**, 13171–13179.
27 Wilson,W.D., Hopkins,H.P., Mizan,S., Hamilton,D.D. and Zon,G. (1994) *J. Am. Chem. Soc.*, **116**, 3607–3608.
28 Cheng,A.J. and van Dyke,M.W. (1993) *Nucleic Acids Res.*, **21**, 5630–5635.
29 Dagle,J.M. and Weeks,D.L. (1996) *Nucleic Acids Res.*, **24**, 2143–2149.
30 Faruqi,F., Krawczyk,S.H., Matteucci,M.D. and Glazer,P.M. (1997) *Nucleic Acids Res.*, **25**, 633–640.
31 Plum,G.E., Pilch,D.S., Singleton,S.F. and Breslauer,K.J. (1995) *Annu. Rev. Biophys. Biomol. Struct.*, **24**, 319–350.
32 Bonham,K. and Fujita,D.J. (1993) *Oncogene*, **8**, 1973–1981.
33 Cooper,J.A. (1990) In Kemp,B. (ed.), *Peptides and Protein Phosphorylation*. CRC Press, Boca Raton, FL, pp. 85–113.
34 Eiseman,E. and Bolen,J.B. (1990) *Cancer Cells*, **2**, 303–310.
35 Faucon,B., Mergny,J.-L. and Hélène,C. (1996) *Nucleic Acids Res.*, **24**, 3181–3188.
36 Musso,M. and van Dyke,M.W. (1995) *Nucleic Acids Res.*, **23**, 2320–2327.
37 Ellerton,N.R. and Isenberg,I. (1969) *Biopolymers*, **8**, 767–786.
38 Scaria,P.V. and Shafer,B.H. (1991) *J. Biol. Chem.*, **266**, 5417–5423.
39 Merguy,J.L., Collier,D., Rougée,M., Garestier,M.T. and Hélène,C. (1991) *Nucleic Acids Res.*, **19**, 1521–1526.
40 Callahan,D.E., Trapane,T.L., Miller,P.S., Ts'o,P.O. and Kan,L.-S. (1991) *Biochemistry*, **30**, 1650–1655.
41 Devlin,R., Studhoime,R.M., Dandliker,W.B., Fahy,E., Blumeyer,K. and Ghosh,S.S. (1993) *Clin. Chem.*, **39**, 1939–1943.
42 Tanha,J. and Lee,J.S. (1997) *Nucleic Acids Res.*, **25**, 1442–1449.
43 Alunni-Fabbroni,M., Pirulli,D., Manzini,D. and Xodo,L.E. (1996) *Biochemistry*, **35**, 16361–16369.